Bandwidth Enhancement of Planar Inverted Cone Antenna

Santanu Mondal[*] and Partha P. Sarkar

Abstract—In this paper, initially a Planar Inverted Cone Metal Antenna (PICMA) is optimized for wideband wireless communication. Finally, a compact Shorted Planar Inverted Cone Metal Antenna (SPICMA) is developed by introducing a shorting strip on the radiating element of optimized PICMA. The PICMA is optimized to operate from 1.7 GHz to more than 20 GHz, and the SPICMA is optimized to extend the operating band from 1.05 GHz to more than 20 GHz resulting in size reduction of 38%. The proposed antenna yields bidirectional radiation pattern in E and H planes. Various characteristics of the antenna have been analyzed using Finite Integration Technique (FIT) based commercial software CST studio. The measured reflection coefficient agrees with the simulated result for the optimized SPICMA.

1. INTRODUCTION

In 2002, Federal communication commission approved the unlicensed ultra-wideband (UWB) that ranges from 3.1 to 10.6 GHz [1]. In the past, conventional configurations such as log periodic, bi-conical and spiral broadband antennas were used extensively for wideband communication systems, but they were not always suitable for compact handheld mobile devices. So, the design of innovative ultra-wideband antennas is demanded to satisfy different specific requirements including size, gain and radiation patterns. Many low cost non-planar metal antennas are reported for ultra-wideband application [2, 3]. In the last few years, some innovative antennas such as printed planar monopole antenna, planar inverted cone antenna (PICA), Vivaldi and volcano antenna have been developed and analyzed for wireless communication related applications to provide ultra-wide bandwidth and omnidirectional radiation pattern [4–11]. The reported planar metal antenna is a modified design of non-planar metal antenna [12, 13].

In this paper, initially a planar antenna is developed where the shape of radiating monopole antenna is constructed similar to that of earlier reported PICA using a metal plate, so named as Planar Inverted Cone Metal Antenna (PICMA). The antenna design with diagram is discussed in detail in Section 2. In Section 3, various antenna parameters such as reflection coefficient, gain, radiation pattern, group delay and antenna factor are obtained by finite integration technique based full wave commercial software CST studio [14]. The simulated results are compared with some measured ones in Section 4. Finally Section 5 presents concluding remarks.

2. ANTENNA DESIGN

The geometry of the proposed SPICMA is shown in Figure 1. The shape of radiating element is constructed similar to that of earlier reported PICA [7–9], and this antenna is designed by a copper plate of thickness 1.2 mm. The proposed antenna is fed by a coaxial to CPW transition to achieve wide impedance bandwidth as shown in Figure 1. The wideband impedance matching has been achieved

* Corresponding author: Santanu Mondal (santanumondal2008@rediffmail.com).
The authors are with the Department of Engineering and Technological Studies, University of Kalyani, Kalyani, WB 741235, India.
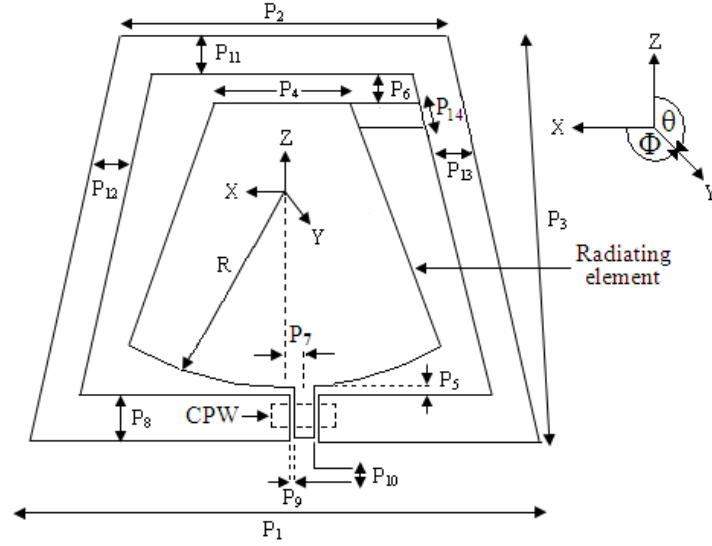
Figure 1. Geometry of the proposed SPICMA.

Table 1. Dimensions of antenna in mm.

P_1	P_2	P_3	P_4	P_5	P_6	P_7	P_8	P_9	P_{10}	$P_{11} = P_{12} = P_{13}$	R
108	68	85.5	26	1.5	5	4	10	1	4	8	41

using trapezoidal ring-shaped ground plane. Other ring-shaped ground planes were also considered, but impedance matching was not good.

Initially, a PICMA is designed, and the optimized design parameters of the proposed PICMA are shown in Table 1. Then a shorting strip is placed in the radiating monopole to develop the SPICMA. The position of the shorting strip is varied so that resonant frequency is decreased. When the shorting strip with width $P_{14} = 5\,\text{mm}$ is placed at the top corner of a radiating element along X axis, the SPICMA shows maximum shift of lower operating frequency, and the new configured antenna operates from 1.05 GHz to above 20 GHz.
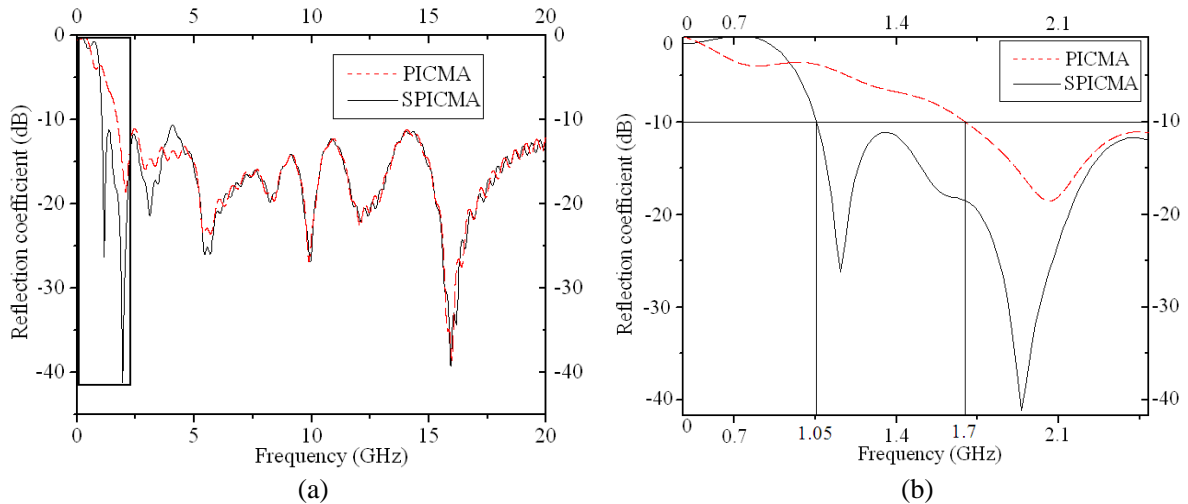
Figure 2. (a) Simulated reflection coefficient vs. frequency plot of PICMA and SPICMA and (b) enlarged marked part of Figure 2(a).

3. SIMULATED RESULTS

The reflection coefficient vs. frequency plots of PICMA and SPICMA are shown in Figure 2(a). Both antennas show ultra-wide impedance bandwidth. Significant shift of lower operating frequency (for reflection coefficient $< -10\,\text{dB}$) in impedance bandwidth is observed after introduction of the shorting strip in PICMA. This portion of the frequency band is marked in Figure 2(a) and emphasized in Figure 2(b) for better visualization. The lower operating frequencies of PICMA and SPICMA are at 1.7 GHz and 1.05 GHz, respectively. So after adding the shorting strip, the size of the antenna is reduced by 38%. Actually, the shorting strip enhances inductive loading that makes this antenna compact and wideband.

Surface current distribution of the antenna dominates near feed section, and outer conductor of the radiating monopole is as shown in Figure 3. This current distribution demonstrates that the dimensions of P_5 and P_9 are very important for achieving compact wideband antenna.

The surface current is not distributed uniformly in the radiating monopole, so different positions of the shorting strip have major impact on input impedance matching. Various positions of shorting strips and their corresponding reflection coefficient characteristics are shown in Figure 4 and Figure 5, respectively. The current density is more at position 3 than that of other positions of the shorting strip, and this position of shorting strip yields significant change of reflection coefficient characteristic of SPICMA from optimized PICMA. The proposed antenna with a shorting strip at position 1 provides
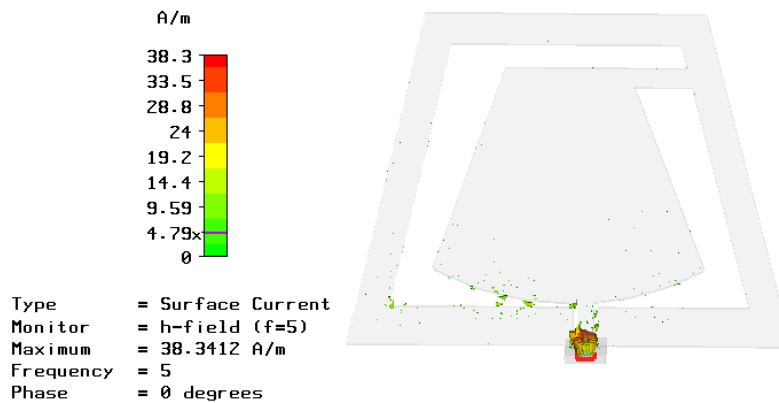
Figure 3. Simulated surface current distribution at the frequency of 5 GHz of SPICMA.
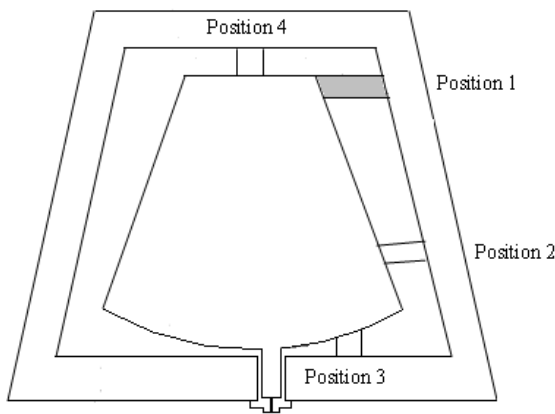
Figure 4. Geometry of the antenna for different positions of shorting strip.
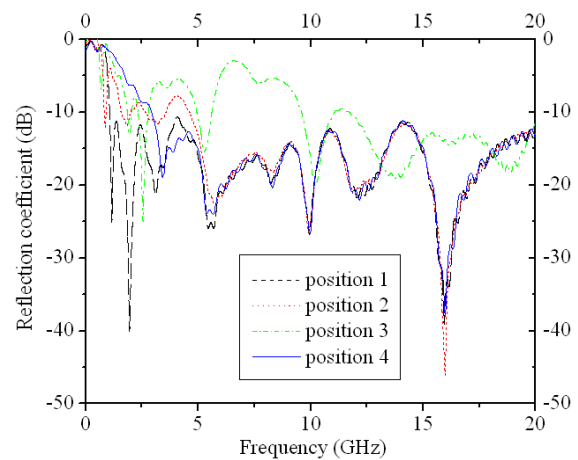
Figure 5. Simulated reflection coefficient vs. frequency plot for different positions of shorting strip of SPICMA.
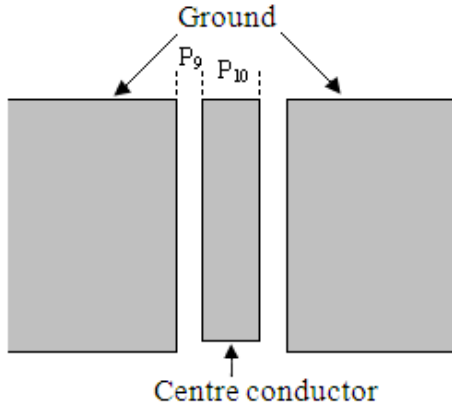
Figure 6. Design of the proposed CPW line.
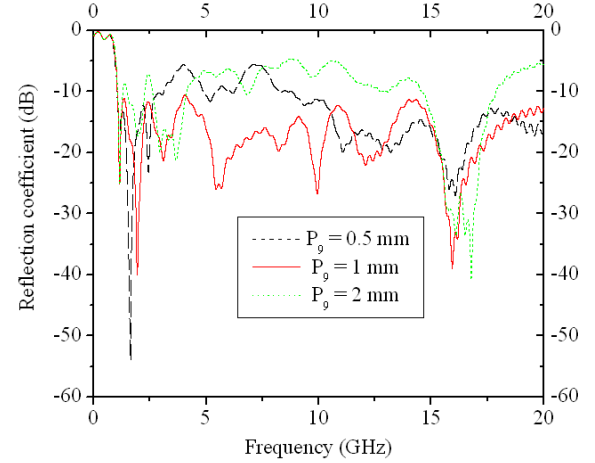
Figure 7. Simulated reflection coefficient vs. frequency plot for different values of P_9 of SPICMA.

(a)

(b)
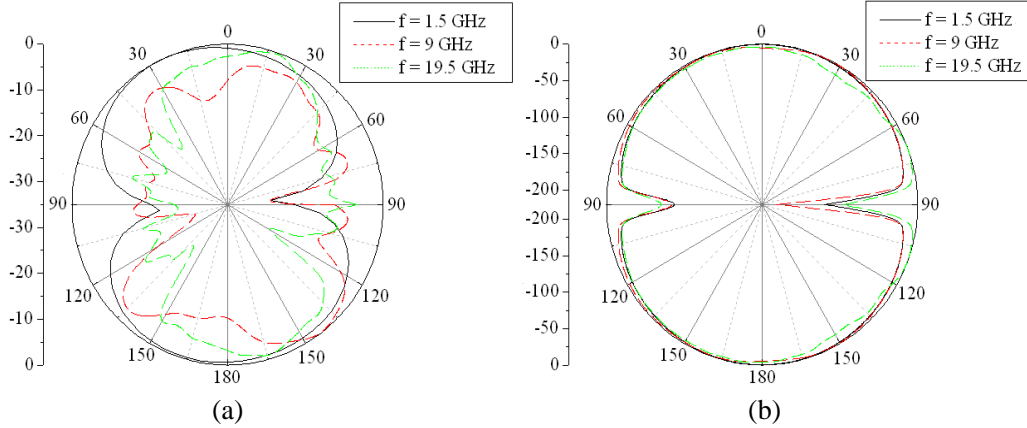
Figure 8. Simulated far field radiation pattern of PICMA at the frequencies of 1.5 GHz, 9 GHz and 19.5 GHz for (a) $\Phi = 0°$, (b) $\Phi = 90°$ plane.

optimized reflection coefficient characteristics as shown in Figure 5. In a similar way, the optimized width of the shorting strip is determined.

The modified CPW line is designed to feed the antenna as shown in Figure 6. The air gap (P_9) between centre conductor and ground of the CPW line takes a vital role to achieve wideband. The reflection coefficient characteristic of the antenna for different values of P_9 is shown in Figure 7, and from this curve the optimized value of P_9 is 1 mm for $P_{10} = 4$ mm.

The optimized PICMA and SPICMA provide stable bidirectional radiation patterns in E and H planes over the operating frequency band. The normalized far-field radiation patterns of optimized PICMA for $\Phi = 0°$ and $\Phi = 90°$ (i.e., E plane) at frequencies of 1.5 GHz, 9 GHz and 19.5 GHz are shown in Figures 8(a) and (b), respectively. The normalized far-field radiation patterns of SPICMA in E plane are shown in Figures 9(a) and (b), respectively. The far-field radiation pattern for $\Phi = 0°$ plane of SPICMA at frequency of 1.5 GHz is tilted compared to PICMA due to the introduction of the shorting strip.

The normalized far-field radiation patterns at $\theta = 90°$ (i.e., H plane) plane of PICMA and SPICMA are shown in Figures 10(a) and (b) respectively. These figures demonstrate the bidirectional pattern of the proposed antenna in azimuth plane. So the radiation patterns of the PICMA and SPICMA are almost the same at higher frequencies.
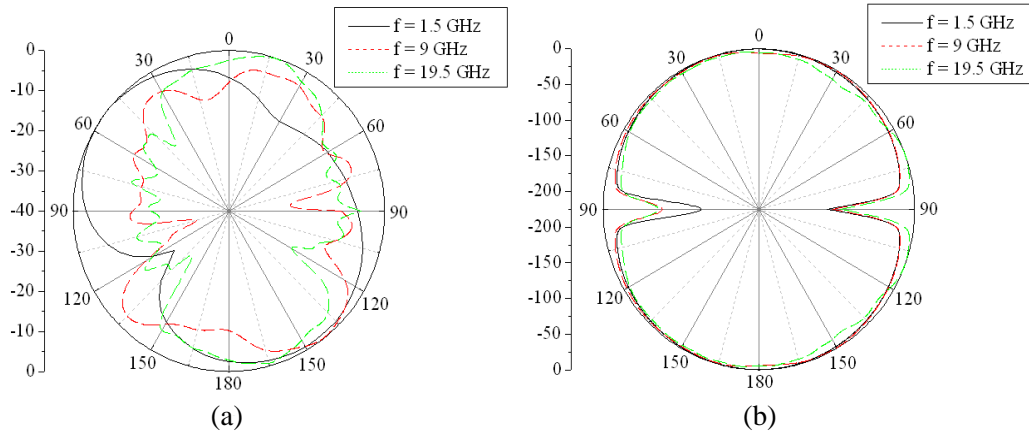
Figure 9. Simulated far field radiation pattern of SPICMA at the frequencies of 1.5 GHz, 9 GHz and 19.5 GHz for (a) $\Phi = 0°$, (b) $\Phi = 90°$ plane.
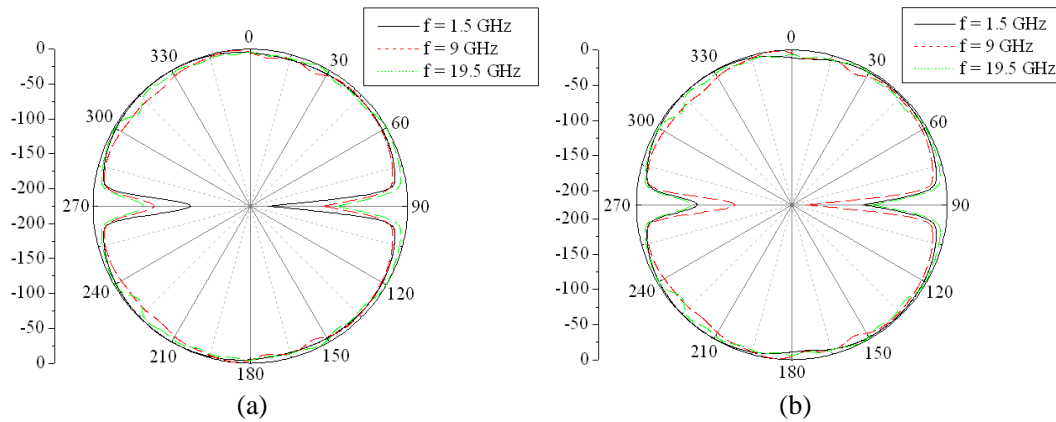
Figure 10. Simulated far field radiation pattern at the frequencies of 1.5 GHz, 9 GHz and 19.5 GHz for $\theta = 90°$ (a) PICMA, (b) SPICMA.
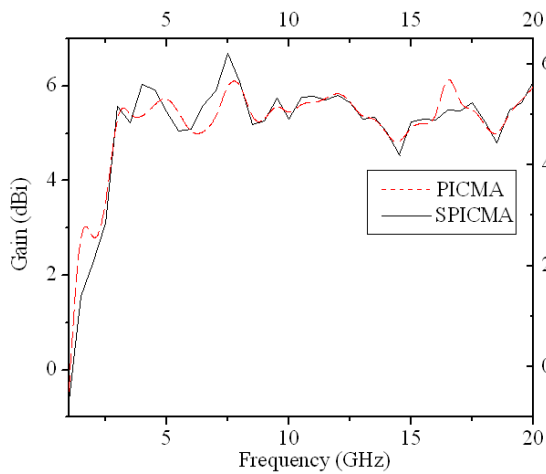
Figure 11. Simulated absolute gain vs. frequency plot of the PICMA and SPICMA.
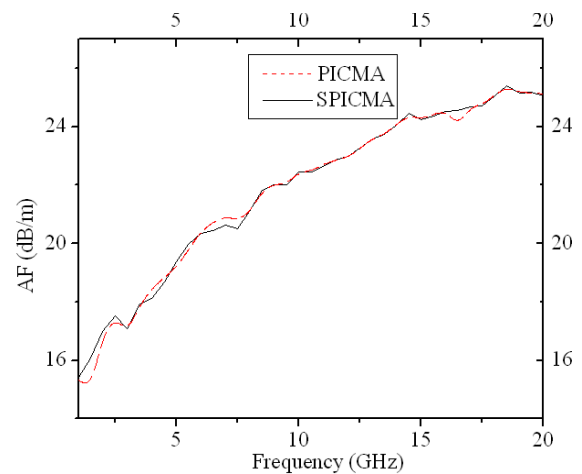
Figure 12. Simulated AF vs. frequency plot of the proposed PICMA and SPICMA.
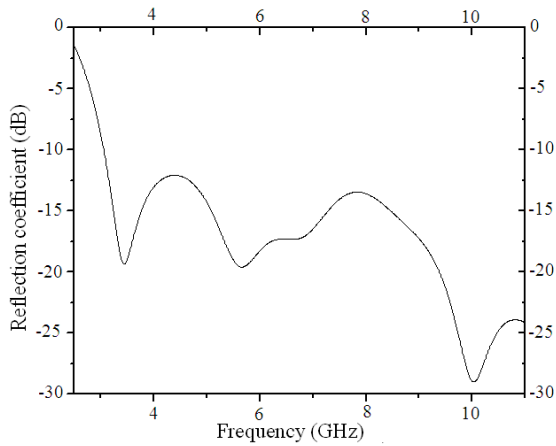
Figure 13. Simulated reflection coefficient vs. frequency plot of ultra-wideband SPICMA.
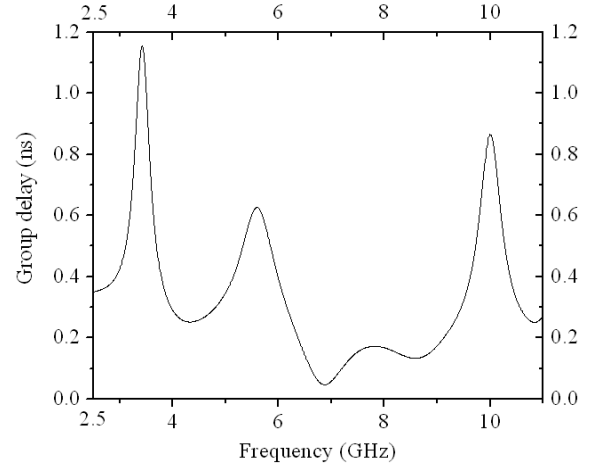
Figure 14. Simulated group delay vs. frequency plot of ultra-wideband SPICMA.

The absolute gain of the PICMA and SPICMA in operating frequency band is shown in Figure 11. The shorting strip of SPICMA does not degrade the gain characteristics.

The simulated absolute gain is used to calculate antenna factor (AF) of the antenna using following relation to check suitability of the proposed antenna for EMC related measurements [15].

$$\text{AF} = 20 \log_{10} \left(\frac{9.73}{\lambda \sqrt{G}} \right) \text{ (dB/m)}$$

where, G = gain of antenna and λ = wavelength.

Variations of AF vs. frequency for PICMA and SPICMA are shown in Figure 12. The antenna factor increases almost monotonically with frequency, which makes these antennas suitable for measurement of radiated emission in their entire operating frequency band.

Frequency scaling property is verified for the optimized SPICMA to check its capability to work at other desired frequency bands. The reflection coefficient vs. frequency characteristic of the SPICMA with $P_1 = 40\,\text{mm}$, $P_2 = 24\,\text{mm}$, $P_3 = 34\,\text{mm}$, $P_4 = 8\,\text{mm}$, $P_5 = 1.5\,\text{mm}$, $P_6 = P_8 = P_{11} = P_{12} = P_{13} = 5\,\text{mm}$, $P_7 = 3\,\text{mm}$, $P_{10} = 2\,\text{mm}$, $P_9 = 1\,\text{mm}$, $P_{14} = 5\,\text{mm}$ and $R = 17.5\,\text{mm}$ is shown in Figure 13. The reflection coefficient of this SPICMA remains below $-10\,\text{dB}$ in the ultra-wideband range. The variation of group delay vs. frequency characteristic of the ultra-wideband SPICMA is shown in Figure 14, and this plot shows that the maximum value of group delay in the ultra-wideband range is $1.15\,\text{ns}$ at $3.43\,\text{GHz}$.

Table 2. Measured gain of the antenna.

	Frequency (GHz)		
	3.5	5	8.5
Gain (dBi)	5.17	4.75	4.38

4. MEASURED RESULTS

The optimized SPICMA has been fabricated using copper plate of thickness 1.2 mm. A photograph of the fabricated SPICMA is shown in Figure 15. The simulated and measured reflection coefficients of the antenna up to 8.5 GHz frequency is shown in Figure 16. Though this antenna has wider bandwidth, the simulated and measured results of the reflection coefficient are shown up to 8.5 GHz due to the frequency limitation of the Agilent E5071B Vector Network Analyzer (VNA). The measured result shows good agreement with the simulated one. Measured reflection coefficient follows simulated reflection coefficient

Figure 15. Photograph of fabricated SPICMA.
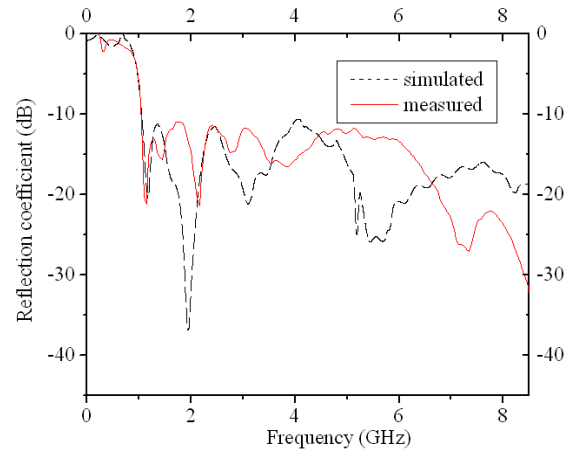
Figure 16. Simulated and measured reflection coefficient of SPICMA.
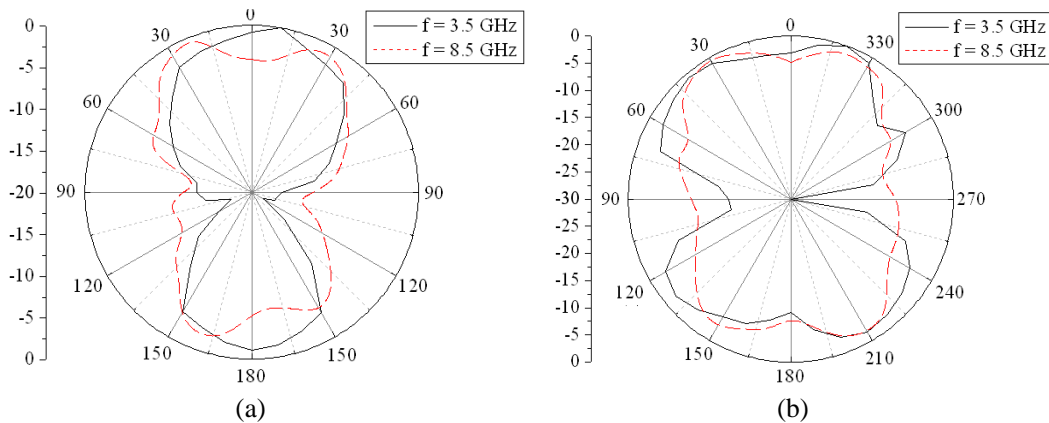
Figure 17. Measured radiation patterns at the frequencies of 3.5 GHz and 8.5 GHz for (a) *E*-plane and (b) *H*-plane.

up to 1.2 GHz. For both the cases the lowest frequency for reflection coefficient < -10 dB occurs at 1.05 GHz, and its value remains below -12 dB. At frequency more than 1.2 GHz, the change in resonance frequency for higher order modes is observed, which may be due to small fabrication errors. The measured absolute gain of the antenna at frequencies of 3.5 GHz, 5 GHz and 8.5 GHz as shown in Table 2 are in good agreement with the simulated results. The measured normalized radiation patterns in E and H planes at frequencies of 3.5 GHz and 8.5 GHz are shown in Figure 17.

5. CONCLUSION

In this study, a compact Shorted Planar Inverted Cone Metal Antenna (SPICMA) is presented. The width and position of a shorting strip are optimized to achieve a size reduction of 38%. The effects of the shorting strip on the characteristics of antenna are analyzed. A modified CPW feed is designed to match with 50 ohm input impedance, and the simulated results show that the impedance bandwidth for $|S_{11}| < 10$ dB of the proposed antenna is from 1.05 GHz to 20 GHz. The bidirectional radiation pattern makes the antenna suitable for repeater application. Due to compact planar structure and wide bandwidth, the proposed antenna may be used for numerous wireless communications including UWB technology.

REFERENCES

1. Schantz, H., *The Art and Science of Ultra Wideband Antennas,* Artech House Inc., 2005.
2. Ghosh, S., "Design of planar crossed monopole antenna for ultrawide-band communication," *IEEE Antennas Wireless Propag. Lett.*, Vol. 10, 548–551, 2011.
3. Lamultree, S. and C. Phongcharoenpanich, "Bidirectional ultra-wideband antenna using rectangular ring fed by stepped monopole," *Progress In Electromagnetics Research*, Vol. 85, 227–242, 2008.
4. Agarwall, N. P., G. Kumar, and K. P. Ray, "Wide-band planar monopole antennas," *IEEE Trans. Antennas Propag.*, Vol. 46, No. 2, 294–295, 1998.
5. Lee, E., P. S. Hall, and P. Gardner, "Compact wideband planar monopole antenna," *Electron. Lett.*, Vol. 35, No. 25, 2157–2158, 1999.
6. Ray, K. P., P. V. Anob, R. Kapur, and G. Kumar, "Broadband planar rectangular monopole antennas," *Microw. Opt. Technol. Lett.*, Vol. 28, No. 1, 55–59, 2001.
7. Hallbjorner, P., C. Shi, A. Rydberg, and K. Karlsson, "Modified planar inverted cone antenna for mobile communication handsets," *IEEE Antennas Wireless Propag. Lett.*, Vol. 6, 472–475, 2007.
8. Shi, C., P. Hallbjorner, and A. Rydberg, "Printed slot planar inverted cone antenna for ultrawideband applications," *IEEE Antennas Wireless Propag. Lett.*, Vol. 7, 18–21, 2008.
9. Suh, S.-Y., W. L. Stutzman, and W. A. Davis, "A new ultrawideband printed monopole antenna: The planar inverted cone antenna (PICA)," *IEEE Trans. Antennas Propag.*, Vol. 52, No. 5, 1361–1364, 2004.
10. Li, T., Y. Rao, and Z. Niu, "Analysis and design of UWB Vivaldi antenna," *International Symposium on Microwave, Antenna, Propagation and EMC Technologies for Wireless Communications*, 579–581, 2007.
11. Yeo, J., Y. Lee, and R. Mittra, "Design of a wideband planar volcano-smoke slot antenna (PVSA) for wireless communications," *IEEE International Symposium on Antennas and Propagation Society*, Vol. 2, 655–658, 2003.
12. Mondal, S. and P. P. Sarkar, "A novel design of compact wideband hexagonal antenna," *Microw. Opt. Technol. Lett.*, Vol. 55, 1–4, 2013.
13. Mondal, S. and P. P. Sarkar, "Design of an extremely wideband planar elliptical metal antenna," *IEEE Antennas Wireless Propag. Lett.*, Vol. 12, No. 1, 1508–1511, 2013.
14. *CST Microwave Studio Manual*, Ver. 10, Computer Simulation Technology, Framingham, MA, 2010.
15. Paul, C. R., *Introduction to Electromagnetic Compatibility*, 2nd edition, Wiley Interscience, 2006.